

## Support Information

### **Angle-independent colours from spray coated quasi-amorphous arrays of nanoparticles: combination of constructive interference and Rayleigh scattering**

**Dengteng Ge<sup>1</sup>, Lili Yang<sup>2,1</sup>, Gaoxiang Wu<sup>1</sup>, and Shu Yang<sup>1,\*</sup>**

<sup>1</sup> Department of Materials Science and Engineering, University of Pennsylvania,  
Philadelphia, PA, 19104, USA

<sup>2</sup> School of Transportation Science and Engineering, Harbin Institute of Technology,  
Harbin, Heilongjiang, 150090, P. R. China

\* Corresponding author: [shuyang@seas.upenn.edu](mailto:shuyang@seas.upenn.edu) (Prof. Shu Yang)

**Table S1.** Volume of TEOS for preparation of silica NPs of different sizes

Diameter of silica NPs (nm)	TEOS (mL)	Polydispersity Index (PDI)
185	0.4	4.2 %
230	1.2	3.5 %
255	1.8	3.3 %
290	2.4	3.8 %
310	2.9	4.2 %
340	3.4	4.5 %

**Table S2.** Properties of solvents used in spray coating

Solvent property	Solvents				
	Water	IPA	Ethanol	Methanol	Acetone
Boiling point (°C)	100	82.5	78.37	64.7	56.3
Vapor pressure (mmHg@20°C)	17.5	21.0	44.2	92.3	182
Surface tension (mN/m@25°C)	72.8	21.7	22.3	22.1	23.1

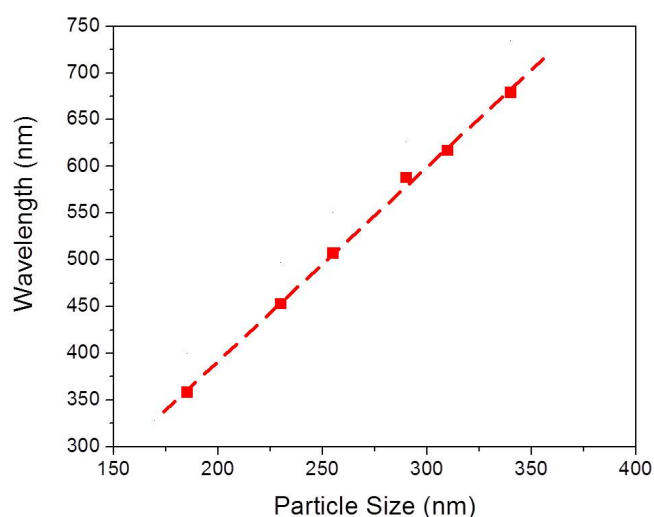


**Fig. S1.** Nanoparticle size vs. the scattering peak position.

## Angle-resolved optical measurement

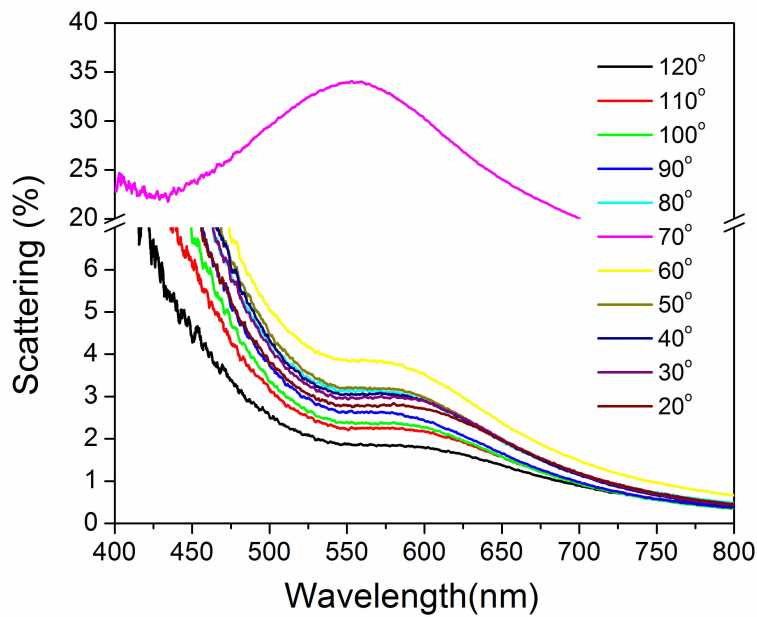


Fig. S2. Scattering spectra of the magenta coating at different angles between the sample surface and the incident light.

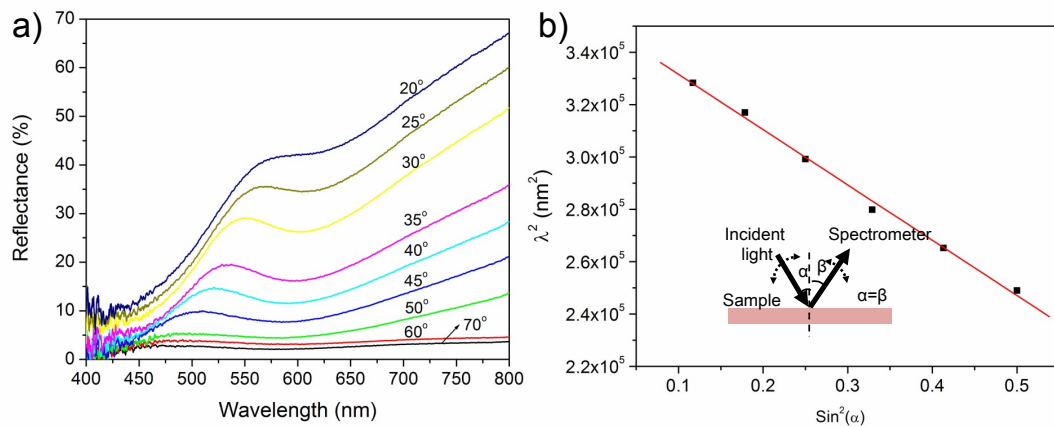


Fig. S3. (a) Specular reflection spectra of the magenta coating with the incident angle,  $\alpha$ , ranging from 20° to 70°. (b) The relationship between  $\lambda^2$  and  $\sin^2\alpha$  from (a).  $\lambda$  is the reflection peak wavelength. The red line is the linear fit. Inset: schematic illustration of the measurement setup.

### Calculation of volume filling fraction of silica NPs

As seen in Fig. S3a, when increasing the incident angle,  $\alpha$ , from  $20^\circ$  to  $70^\circ$ , the intensity of specular reflection decreased, accompanied with a blue shift of the reflection peak. This phenomenon was similar to the observation from a colloidal crystal except that the peaks were much broader and weaker here, suggesting that the reflected light was dominated by the constructive interference of the scattered light while the short-range order considerably attenuated the scattered light. As seen from the cross-sectional SEM image of the quasi-amorphous structure shown in Fig. 2c, the particles were organized with a certain degree of ordering. It was believed that the scattering peak of quasi-amorphous structure at the specular angle was due to interference of reflected light from the ordered colloidal layers.

According to the Bragg-Snell's law, the relationship between the reflection peak wavelength  $\lambda$  and incidental angle  $\alpha$  of an ordered structure is

$$\lambda_{\max} = 2d(n_{\text{eff}}^2 - \sin^2 \alpha)^{1/2} \quad (1)$$

where  $d$  is the (111) plane interplanar spacing and  $n_{\text{eff}}$  is the effective refractive index. As seen in Fig. S3b, there is a linear relationship between  $\lambda^2$  and  $\sin^2 \alpha$  in the spray coated film, suggesting that the spectra of quasi-amorphous structures at specular angles still fit the Bragg-Snell's law.

From the linear fitting, we obtained  $d = 229.8$  nm and  $n_{\text{eff}} = 1.29$  for the angle-independent magenta coating from 310 nm-silica NPs. Here,

$$n_{\text{eff}} = n_{\text{silica}} \phi_{\text{silica}} + n_{\text{air}} \phi_{\text{air}} \quad (2)$$

where  $n_{\text{silica}} = 1.45$ ,  $n_{\text{air}} = 1$  and  $\phi$  is the volume filling fraction. Accordingly, we derived the volume filling fraction of silica NPs,  $\phi_{\text{silica}} = 0.65$ .

For an fcc colloidal crystal consisting of spherical particles,  $\phi_{\text{silica}}^{\text{fcc}} = 0.746$ . It has been reported that for an amorphous structure by drop-casting of mixed polystyrene particles,  $\phi^{\text{am}} = 0.5$ .<sup>1</sup> From  $0.5 < \phi_{\text{silica}} = 0.65 < 0.746$ , it is clear that the angle-independent colored film in our system is quasi-amorphous with both ordered and random structures.

### Calculation of the intensity of Rayleigh scattering

Rayleigh scattering intensity  $I'$  of a single particle from a beam of unpolarized light of wavelength  $\lambda$  and intensity  $I_0$  is given by

$$I' = I_0 \frac{1 + \cos^2 \theta}{2S^2} \left( \frac{2\pi}{\lambda} \right)^4 \left( \frac{n^2 - 1}{n^2 + 2} \right)^2 \left( \frac{D}{2} \right)^6 \quad (3)$$

where  $\theta$  is the scattering angle,  $S$  is the distance between the particle and the detector,  $n$  is the index of refraction of the particle,  $D$  is the diameter of the particle.

Rayleigh scattering of the overall particle film can be defined as

$$I / I_0 = (NI') / I_0 \quad (4)$$

Here,  $N$  is the number of particles per unit volume illuminated by the incident light and it is given by

$$N = \frac{\phi Ah}{\pi d^3 / 6} \quad (5)$$

where  $A$  is the area of incident light beam ( $4 \text{ mm}^2$  in our experiments),  $h$  is the thickness of NP films,  $\sim 5 \text{ }\mu\text{m}$  from Fig. 2c.

Given  $S = 100 \text{ mm}$ ,  $\theta = 90^\circ$  and  $\phi = 0.65$ , which was calculated previously, we plotted the calculated Rayleigh scattering intensity from the overall NP films vs. wavelength as seen in Fig. 5a.

### Calculation of reflectance intensity at the interface

The reflectance at the interface between two media under normal incident light is

$$R = \frac{(n_1 - n_2)^2}{(n_1 + n_2)^2} \quad (6)$$

where  $R$  is reflectance of the interface between media 1 and media 2;  $n_1$  and  $n_2$  are the refractive indices of media 1 and media 2. As seen in Fig. 6c, there were three layers under the quasi-amorphous array of NPs, including glass substrate, the interlayer and the background. In our research, black polypropylene (PP) was used as background and air or water was the interlayer. Here,  $n_{\text{glass}}=1.45$ ,  $n_{\text{air}}=1$ ,  $n_{\text{pp}}=1.47$ ,  $n_{\text{air}}=1$  and  $n_{\text{water}}=1.33$ . The reflectance at the interface between them according to Eq. (6) is  $R_{\text{glass-air}}=3.3\%$ ,  $R_{\text{pp-air}}=3.6\%$ ,  $R_{\text{glass-water}}=0.18\%$ ,  $R_{\text{pp-water}}=0.25\%$

### Color fitting

The apparent colors as a function of wavelength were obtained from the chemwiki.<sup>2</sup> From the transmission spectra of NP films shown in Fig. S4, the peaks of

constructive scattering were 453 nm, 507 nm, 588 nm, 617nm, and 679 nm, respectively, for NP size of 230 nm, 255 nm, 290 nm, 310 nm and 340 nm, respectively. The corresponding colors arising from the interference scattering peaks, referred as spectra colors, were shown in Fig S4. Accordingly, the colors arising from the Rayleigh scattering were referred as Rayleigh scattering colors. The Rayleigh scattering color was obtained from the real color of the sprayed coating from 100 nm silica NPs because there was only Rayleigh scattering in this coating. It should be noted that, however, the intensity of Rayleigh scattering increases with the increase of silica NPs size. The intensities of the interference scattering peaks of samples varied from sample to sample (Fig. S4). To normalize the scattering intensity, we measured the transmittances ( $T$ ) of each sample (see Table S3). The intensity of omnidirectional scattering at the interference scattering peak was estimated as  $I-T$  due to the negligible light absorptions of silica. It can be seen that the intensity at the constructive scattering peak decreased when increasing the particle size, suggesting that the intensity ratio between the constructive interference and Rayleigh scattering is different for different NPs coatings.

To mix these two colors and match the real colors appeared in our samples, the brightness of the spectrum color was adjusted using Adobe Photoshop, where the exposure offset was arbitrarily set to decrease at a step of 0.5 from the constructive scattering peaks at 453 nm, 507 nm, 588 nm, 617nm, and 679 nm, respectively (see Fig. S5). Using Adobe Photoshop and simply mixing the colors according to color addition theory, we obtained the colors closely matched with those appeared from the samples shown in Fig. 2.

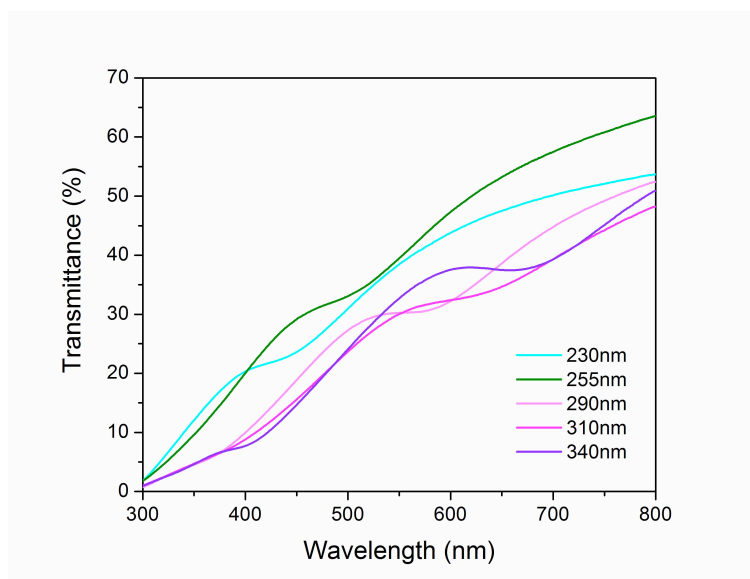


Fig. S4. Transmittance of coloured coatings obtained from silica NPs of different diameters.

**Table S3.** Position, Transmittance ( $T$ ) and  $I-T$  at the scattering peaks

Size of NPs	230 nm	255 nm	290 nm	310 nm	340 nm
scattering peak	453 nm	507 nm	588 nm	617 nm	679 nm
Transmittance at the scattering peak ( $T$ )	23.9%	34.7%	30.4%	32.9%	37.6%
$I-T$	76.1%	65.3%	69.6%	67.1%	62.4%

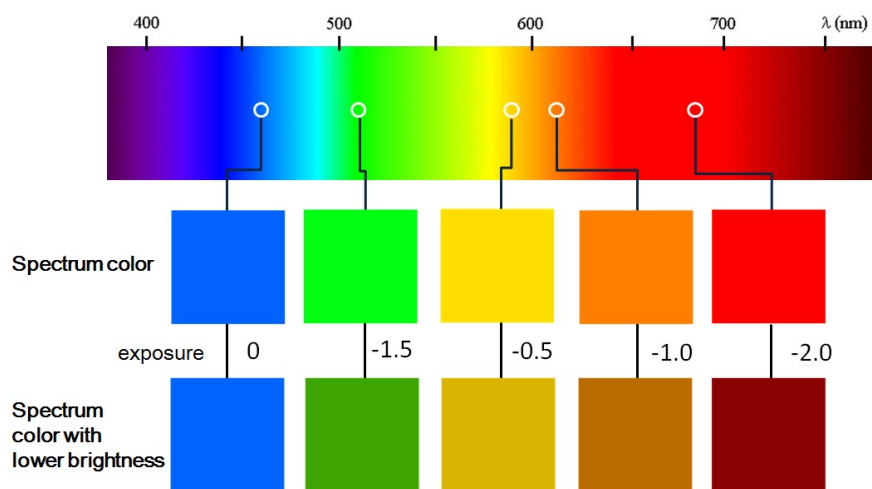


Fig. S5. Spectrum colors according to different constructive scattering peaks

The photos of the quasi-amorphous arrays on a white paper, a black PP film, and a black PP film with a water layer were summarized in Table S4. The hue (H), saturation (S) and brightness (B) of each color can be obtained using Adobe Photoshop. From Table S4, it could be seen that the saturation of the color was highly enhanced after injecting the water layer in between the glass and the black PP film.

**Table S4.** Hue, saturation and brightness of the colors (data from Photoshop) produced from quasi-amorphous NP arrays on different backgrounds

a) Background: White paper								
	H (°)	190	180	173	103	60	48	20
	S (%)	7	3	5	4	5	3	1
	B (%)	66	71	73	73	74	72	68
b) Background: black PP film								
	H (°)	84	168	138	80	40	27	23
	S (%)	3	2	7	15	23	19	13
	B (%)	66	69	75	72	84	79	72
c) Background: black PP film with a water layer								
	H (°)	219	214	195	112	24	348	274
	S (%)	54	53	42	29	32	24	17
	B (%)	41	59	58	46	76	57	50

**Reference:**

1. J. D. Forster, H. Noh, S. F. Liew, V. Saranathan, C. F. Schreck, L. Yang, J. G. Park, R. O. Prum, S. G. J. Mochrie, C. S. O'Hern, H. Cao and E. R. Dufresne, *Adv. Mater.*, 2010, 22, 2939-2944.
2. [http://chemwiki.ucdavis.edu/Inorganic\\_Chemistry/Crystal\\_Field\\_Theory/Virtual%3A\\_Electronic\\_Structure/Color\\_in\\_Gems](http://chemwiki.ucdavis.edu/Inorganic_Chemistry/Crystal_Field_Theory/Virtual%3A_Electronic_Structure/Color_in_Gems)